Indoor mobile robot self-localization based on a low-cost light system with a novel emitter arrangement

ROBOMECH Journal

RESEARCH ARTICLE

Open Access

CrossMark

Indoor mobile robot self-localization based on a low-cost light system with a novel emitter arrangement

Jun Wang* and Yasutake Takahashi

Abstract

This paper proposes a low-cost infrared (IR) LED system with a novel arrangement that enables the self-localization of an indoor mobile robot. The proposed system uses only low-cost IR LED emitters installed on the ceiling of a building and low-cost IR receivers, each equipped with a photodiode, located on top of the mobile robot for detection. The IR LEDs, which are driven by an on-off keying modulator with various frequencies, are used as active landmarks. The mobile robot localizes itself based on the IR LED signals it receives. Although it would be desirable to assign a unique ID to each emitter, this would be difficult to realize because of the limited number of available frequencies and the production cost resulting from the use of independent microcontrollers. Therefore, we designed a novel landmark configuration consisting of an IR LED array with unique ID-encoding capabilities based on a combination of different frequencies and the repeated use of each ID encoding LED to address the problem of limited frequencies. The novel landmark arrangement reduces the costs associated with production, ID encoding, and computation. A Monte-Carlo localization method with a belief function is utilized to estimate the position and orientation of the mobile robot based on the decoded ID information and received signal strength. The proposed system was tested in a real environment and the experimental results confirmed the validity and accuracy of the system and method.

Keywords: Indoor mobile robot, Infrared sensor, ID combination, Non-unique ID, Monte-Carlo localization

Introduction

Indoor mobile robots are currently being utilized to perform various tasks. One of the fundamental requirements for an indoor mobile robot is a localization technique, which is necessary to estimate the position and orientation of the mobile robot based on the measurements and prior knowledge such as a map of the environment, its initial position, or known landmarks. Localization is required because it is difficult for any indoor mobile robot to perform its assigned tasks independently without accurate knowledge of its position in the environment.

Several kinds of sensors have been used for the self-localization of indoor mobile robots, such as WiFi positioning, laser range finders (LRFs), the radio frequency

identification (RFID) system, vision sensors, ultrasonic positioning, Bluetooth technology, visible light communication (VLC) technology, and an infrared (IR) emitter and receiver. Although the hardware required to support WiFi [1, 2] and Bluetooth [3, 4] is easily integrated into mobile devices, both WiFi- and Bluetooth-based positioning systems are easily disturbed because interference by other signals affects their accuracy. Ultrasonic [5, 6] and LRF [7, 8] positioning systems have the advantage of high positioning accuracy and a relatively simple system structure. However, sensors of both of these two types are unable to locate a mobile robot accurately if the robot is surrounded by unknown moving objects. The use of LRFs is also restricted in an environment with transparent walls, which are currently widely used in indoor environments. An RFID system can provide accurate localization with a dense and reasonable configuration of IC tags [9, 10]. However, this technology needs a large amount of preparation work, e.g., building a map of

*Correspondence: jwang@ir.his.u-fukui.ac.jp
Department of Human and Artificial Intelligent Systems, Graduate School of Engineering, University of Fukui, 3-9-1, Bunkyo, Fukui, Japan

the IDs and the positions of the RFID tags. Moreover, an RFID reader is relatively expensive. A vision sensor-based positioning system [11] can realize the self-localization of a mobile robot without reforming the environment and is conducive to human-computer interaction. However, the vision sensor is adversely affected by changes in the illumination and environmental conditions.

Although the LEDs need to be reformed, the IR system [12–14] and VLC technology [15, 16] have the advantages of a stable signal, fast response, high confidentiality of information, and they are less affected by environmental change. These characteristics are useful for the self-localization of an indoor mobile robot and prompted us to use an IR system in this research to locate the indoor mobile robot.

Most IR-system-based self-localization applications for an indoor mobile robot depend on known artificial landmarks, which can be classified into active and passive. Passive landmarks are fabricated with IR light-reflecting materials without using any external power. A CMOS IR camera and an IR LED array are integrated into the mobile robot to locate the robot based on the detected passive landmarks [17, 18]. IR emitters are usually used as active landmarks [19, 20] that are positioned at stationary locations and continuously emit an IR signal. This signal is received by the IR receiver located on the mobile robot, which uses the information to estimate its location.

To the best of our knowledge, most IR-system-based self-localization approaches use a unique ID to encode the landmarks. This means that some mobile robot localization techniques are inappropriate for a large indoor environment because of the limited availability of IDs and the associated high production cost. However, many mobile robots are intended for operation in large public indoor environments, e.g., museums, supermarkets, large exhibition centers, theaters, large dining halls, large conference rooms, and large sports complexes. Therefore, there is considerable demand for an affordable indoor mobile robot self-localization system capable of supporting an adequate number of available IDs.

In this paper, we propose an indoor mobile robot self-localization system with a novel arrangement of active landmarks with the aim of solving the problem of limited IDs and of reducing the production, ID, and computational costs. We planned to achieve this by using IR LEDs as active landmarks that emit modulated IR signals continuously. The ID of active landmarks is often driven by an on-off keying (OOK) modulator, which is stored in the memory and is used to generate the modulation signal by the microcontroller. Encoding the ID of the emitter by 32-bit information is almost sufficient for a large environment. However, the decoding process is adversely affected by overlapping signals. The IDs used in this

research are encoded by the frequencies of the IR signal emitted by the IR LEDs.

Two types of active landmarks are used in this research. The first type is an IR LED array encoded by a unique ID with a combination of different frequencies. The other is an IR LED encoded by a repeatedly used ID with a single frequency. All of the IDs used in this research are designed by using only nine different frequencies; however, our combined method offers 511 available IDs at most. These 511 available IDs can be used in a larger environment with accurate self-localization estimation by using a novel configuration in which the unique IDs are combined with those from some landmarks in the environment with IDs generated by repeated encoding. This novel configuration is also useful for an indoor mobile robot self-localization system based on passive landmarks.

The active landmarks are installed on the ceiling as this arrangement would minimize disturbance of the signals by obstacles. Two receivers, each equipped with a photodiode, are positioned on top of the mobile robot. The robot utilizes the receivers to scan the IR signals emitted from the landmarks and realizes self-localization based on the prior known positions of the detected landmarks. Because some IDs are used repeatedly in the environment, we propose to use a belief function to compute the probability of each landmark encoded by a repeatedly used ID. The position of the landmark with the largest belief is used to estimate the robot location. We also utilize the received signal strength (RSS) method to realize a more accurate estimation. Instead of using the Lambertian radiant intensity [21] to compute the relationship between the distance of the detected IR LED and the photodiode with the output voltage of the receiver, we used a machine-learning method to obtain a formula based on the experimental data.

The Monte-Carlo localization (MCL) method [22] is used in combination with the belief function to estimate the position and orientation of the mobile robot. The experimental results we obtained when testing the proposed system in a real experimental environment confirmed the validity of the system. The key contributions of this study are as follows.

1. A low-cost localization system based on IR emitters and receivers for an indoor mobile robot was developed.
2. Additional unique IDs are made available by using a combined method that solves the problem of limited IDs.
3. A novel configuration that combines unique ID encoding landmarks with repeated ID encoding landmarks is proposed to improve the estimation accu-

racy and reduce the production, ID, and computational costs.

4. An MCL method with a belief function is proposed to estimate the position and orientation of a mobile robot in an environment with landmarks that employ repeated ID encoding.

Related work

Many localization techniques have been developed for indoor mobile robots. Surveys, including comparisons, of indoor mobile robot localization techniques were presented in [23–27]. Our paper mainly presents an analysis of existing approaches based on the IR system and their comparison with the proposed system.

Several applications based on an IR system using passive landmarks for indoor mobile robot localization have been developed. The Hagisonic StarGazer localization system [28] is one of the widely used passive landmark-based localization systems for indoor mobile robots. This system was experimentally evaluated by Ul-Haque et al. [29], who found the system to be reliable, accurate, robust, and affordable. They also determined the position and orientation accuracy to be reasonably high based on their experimental data. Oh et al. [17] developed an indoor localization system based on the Hagisonic StarGazer localization system. They also evaluated this system and found several types of deviations from the actual values. They decreased the errors that occurred during the study by using an optimal arrangement of landmarks and an adaptive extended Kalman filter. Their experimental results attested to very good accuracy.

Lee [18] developed a localization system that utilized the same principle of reflective landmarks as the Hagisonic StarGazer localization system. Artificial landmarks were created using films coated with IR light-reflecting material. The landmarks were shaped in the form of right-angled equilateral triangles and installed on the ceiling. A CMOS camera with a USB interface was used to capture images of the landmarks. The CMOS camera achieved this by capturing two successive images with and without IR light illumination to show the IR light-reflecting landmarks clearly. Image distortion was corrected by using the kinematic relation. The position and orientation of the camera could be estimated based on the prior known positions of the detected landmarks. A pan/tilt mechanism was also used to provide a wider area of coverage to enable the number of required landmarks to be reduced.

As presented in [29], the Hagisonic StarGazer localization system costs nearly $1750 for an area sized approximately 2000 m^2. This amount includes the cost of the localization sensor ($1400) and the cost of the passive landmarks attached to the ceiling. The cost of a passive landmark of the type with an HLD1-L 4×4 grid is approximately $3.52. Because of the considerable cost of the localization sensor, this localization system is unsuitable for an environment in which multiple mobile robots operate together, which is typically the case in large-scale environments, and where multiple localization sensors are needed. The passive landmarks used in the Hagisonic StarGazer localization system are inexpensive and easily installed. These are good characteristics for a large environment. However, the ability to support thousands of unique landmark IDs is not suitable to large-scale environments, whereas our proposed system offers a larger number of unique IDs and utilizes repeated IDs. Another comparable system [18] uses even fewer available unique landmark IDs than the Hagisonic StarGazer localization system.

An IR signal emitter and detector are essential components in a localization system based on active landmarks. Most approaches utilized an emitter as the active landmark. Krejsa and Vechet [19] used IR beacons that only provided information about the bearing. Their system consisted of placing beacons with known positions in the environment. The signals from these beacons were then detected by a scanner device placed on top of the robot chassis. The scanner consisted of 16 receivers placed in a circle covering the entire range of 360°. The location of the robot was estimated based on the extended Kalman filter (EKF) method, which combines the odometry and bearing information with the initial position of the mobile robot. Our approach involved the use of two receivers capable of obtaining both the bearing and strength information to improve the accuracy. Especially, the robot in our approach estimates its position autonomously without having known its initial position.

Lee and Song [30] used unique ID encoding IR LEDs as artificial landmarks for mobile robot localization. The placement of different ID encoding LEDs on the ceiling made it possible to divide the robot activity area into several sectors with each sector set to have a unique identification. The robot was equipped with a receiver when moving across the floor. This enabled the robot to estimate its position with large uncertainty based on sectors with a large size. They presented an algorithm that fuses both the odometry and the IR ID information such that the magnitude of the uncertainty was reduced. However, an appropriate starting point and unit length are needed and overlapped signals cannot be analyzed with the binary information identification. Moreover, the uncertainty can be decreased more effectively by using the RSS method, which we use in our approach.

Some studies also attempted to use the receiver as the active landmark. Gorostiza et al. [31] developed a sensorial system. Their system was capable of measuring

different phase-shifts in a sinusoidally modulated IR signal transmitted by the robot. The system consisted of one emitter set on the robot and a single photo-detector for each receiver installed on the ceiling. Different distances were obtained from these phase-shifts, and the position of the robot was estimated by hyperbolic trilateration. Their experiments determined the locating precision to be below 10 cm. Replacing the emitter and installing the receiver in the ceiling with reasonable configuration indeed succeeded in avoiding the ID limitation. However, this system requires a backstage controller to receive the information from all the receivers and transmit the corresponding positional data to each mobile robot after estimating the positions of all mobile robots based on the received information. This considerably increases the computational cost in a large-scale environment with multiple mobile robots.

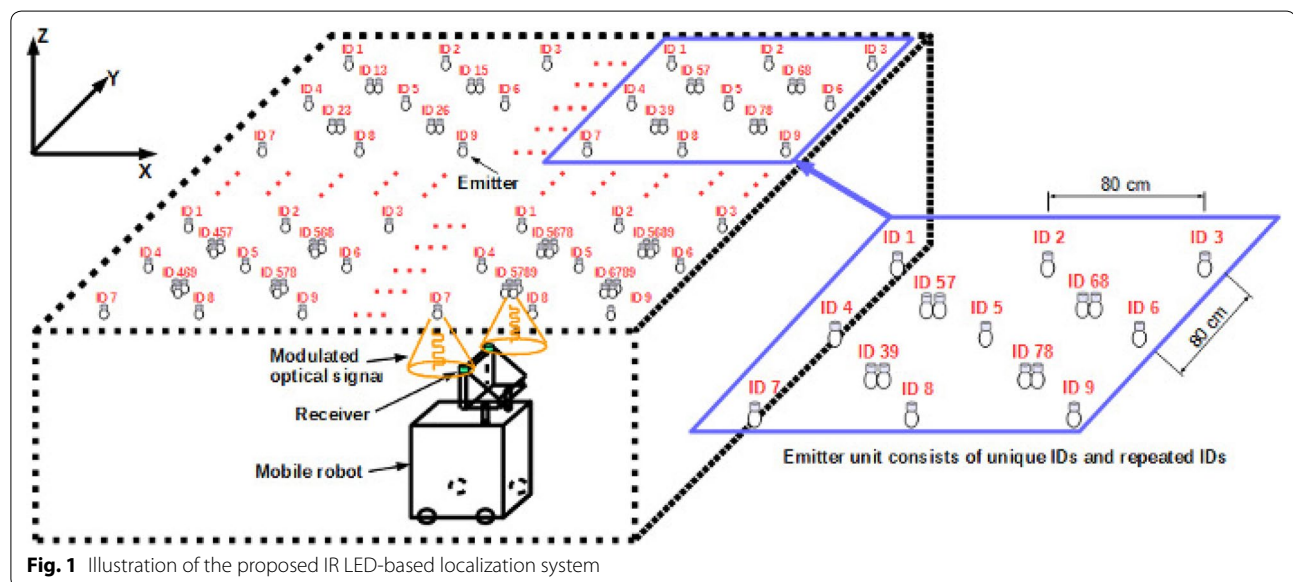## IR system for the self-localization of an indoor mobile robot

The proposed system consists of the following main components: two types of emitters and two receivers. The emitters are used as landmarks and continuously transmit a modulated IR signal. The receiver obtains and amplifies the IR signal to recognize the ID and signal strength of the detected emitter. The estimation of the position and orientation of the mobile robot is based on the prior known positions of the detected emitters. The proposed IR LED-based localization system is illustrated in Fig. 1.

Modulated IR LEDs are used as landmarks and are installed on the ceiling. We use a combination of frequencies to generate additional IDs. This circumvents the
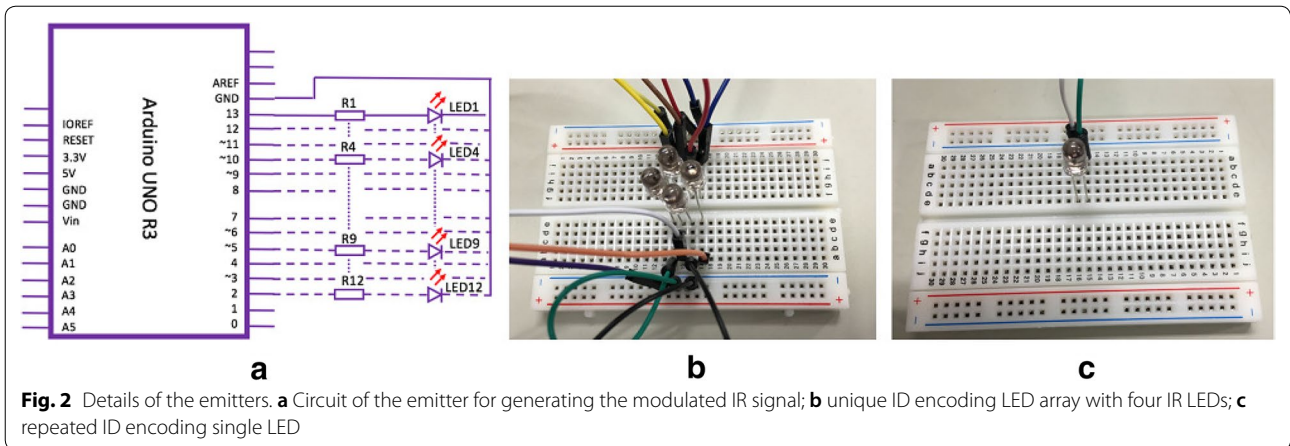
problem caused by the availability of a limited number of IDs. Some IDs are used as repeated IDs to ensure the limited IDs can be used in a larger environment. In consideration of the production cost, a single IR LED with a single frequency is used as the repeated ID encoding emitter. The IR LED array encoded by the combination of multiple frequencies is used as the unique ID encoding emitter. Figure 2b shows a unique ID encoded with an IR LED array consisting of four LEDs. The other type of IR LED performs repeated ID encoding as shown in Fig. 2c.

The two types of emitters are installed in a lattice pattern as shown in Fig. 1. The unique ID encoding emitter is positioned in the center of the square formed by four repeated ID encoding emitters. This arrangement is similar to that used in a cellular network. Utilization of this configuration enables the robot to estimate its position and orientation and to start anywhere in the designated area. The use of repeated ID encoding emitters results in landmarks being detected more frequently, thereby improving the accuracy of the robot location without the need to consume unique IDs. The detection range of the receiver is within 280 mm. The interval between two adjacent emitters of the same type is set to 800 mm to ensure the receiver is able to detect the IR signal frequently. This is intended to improve the accuracy of the robot location but prevent the receiver from capturing signals from different emitters at the same time. The interval between the unique ID encoding emitter and the repeated ID encoding emitter is approximately 566 mm.

The ID of the emitter driven by the on-off keying (OOK) modulator is stored in the memory and then used by the microcontroller to generate the modulation signal as shown in Fig. 2a. The IDs are defined by the

Fig. 1 Illustration of the proposed IR LED-based localization system

Fig. 2 Details of the emitters. **a** Circuit of the emitter for generating the modulated IR signal; **b** unique ID encoding LED array with four IR LEDs; **c** repeated ID encoding single LED
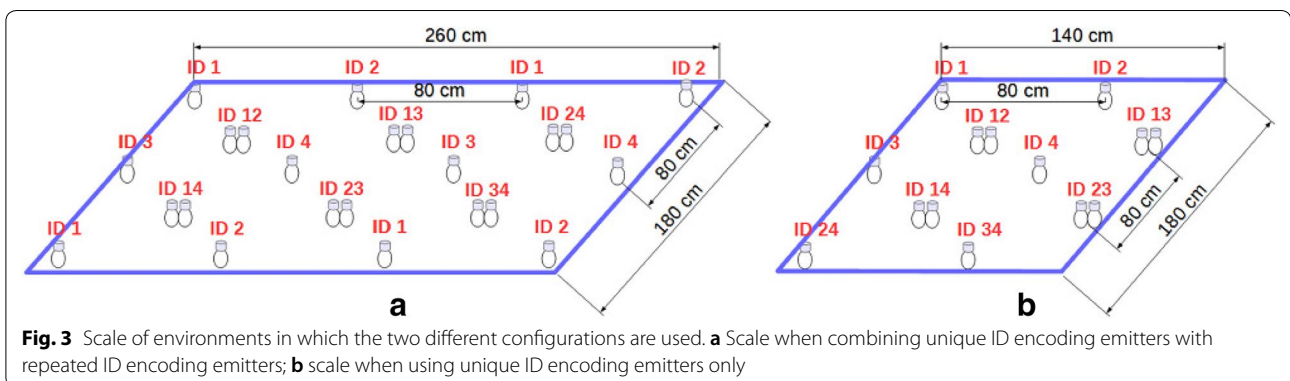
frequencies of the emitted signals. Because of the limited availability of frequencies in an actual environment, using a system with frequency-based ID in a large-scale environment would be prohibitive. Therefore, we propose the use of a combination of different frequencies to define the ID, and prove the validity of this method here. A microcontroller with 20 different frequencies and four digital output pins can provide $\sum_{n=1}^{4} {}_{20}C_n = 6195$ unique IDs by using the combined method. This multiple, which is approximately 30 times more than the number of raw available frequencies, could be improved by providing additional available frequencies and digital output pins.

In this work, nine different frequencies, which are listed in Table 1 together with their corresponding code, are used to generate the IDs of the emitters; for example, ID 57 shown in Fig. 1 signifies the combination of code 5 and code 7. Identification of an LED array by ID 57

indicates that one LED is modulated by a frequency of 550 Hz, whereas the other is modulated by a frequency of 850 Hz. The combined method allows $\sum_{n=1}^{9} {}_{9}C_n = 511$ IDs to be obtained by employing a microcontroller with nine available digital output pins. The uncertainty of the location of the robot increases as the interval between emitters increases. Our proposed solution addresses this problem by using a configuration that combines unique ID encoding emitters with repeated ID encoding emitters rather than simply using unique IDs. The use of repeated IDs in an environment in which the self-localization of a mobile robot was feasible was proposed by Wang and Takahashi [32]. The configuration proposed in this paper allows us to use the same quantity of available IDs to achieve the same location accuracy in larger environments. As shown in Fig. 3, there are ten available IDs and the interval between the emitters used in these two

Table 1 Frequencies used to generate the IDs

Code	1	2	3	4	5	6	7	8	9
Frequency (Hz)	100	150	250	350	550	650	850	950	1150

Fig. 3 Scale of environments in which the two different configurations are used. **a** Scale when combining unique ID encoding emitters with repeated ID encoding emitters; **b** scale when using unique ID encoding emitters only

configurations is the same. The scale of the environment in which the unique ID encoding emitters are combined with the repeated ID encoding emitters in Fig. 3a is larger than that involving the use of unique ID encoding emitters in Fig. 3b. In the proposed system, the robot processes self-localization without the need for initialization with a default value. Especially, emitters with the same ID can be driven by one microcontroller, thereby reducing the production cost.

The circuit of the receiver, of which two are located on top of the mobile robot, is shown in Fig. 4a. The intensity of the received light is reflected as the voltage of R1 by using the reverse bias circuit with the photodiode. A non-inverting amplifier is used to amplify the voltage signal to enable the IR signals to be analyzed. The receiver then transforms this optical signal into an electrical signal, which is subsequently used to identify the detected emitter. Figure 4b shows an image of the receivers with the two photodiodes set on top of the mobile robot, as used in this work. The geometric relationship between the receivers and the robot in 2D space is shown in Fig. 4c.

The IR LED and the photodiode used in the proposed system have the part numbers OSI5LA5113A and TPS 705, respectively. An Arduino UNO R3 is used to drive the LEDs and link with the receiver circuits.
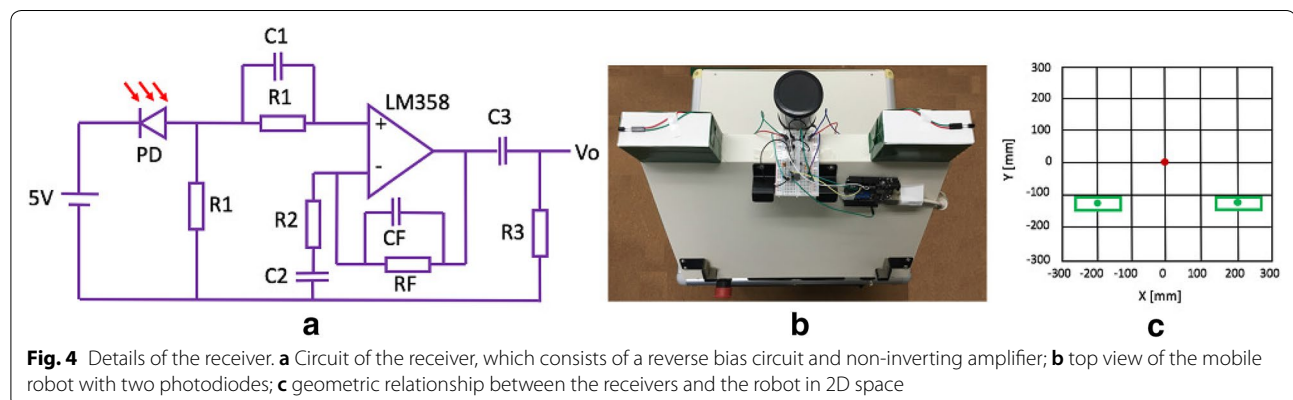
Self-localization of the indoor mobile robot based on the proposed system

In this research, the self-localization of the mobile robot is estimated by the MCL method with a belief function. This section is divided into four parts. The first describes the recognition of the detected emitter. The receivers on the robot transform the received optical signal to an electrical signal. An emitter with a unique ID can easily be recognized by analyzing the frequencies of the received signals and by comparing them with the prior known ID

database. However, repeated ID encoding emitters need a belief function to determine which emitter is being detected with the detected ID. The second part explains the calculation of the distance between the receiver and the detected emitter in the horizontal plane based on the strength of the received signal which is used as the observation model. Rather than using the Lambertian radiant intensity, we use a machine-learning method to obtain a formula to represent the relationship between the strength of the voltage signal generated on the receiver with the distance of the receiver and the detected emitter. This formula, which was derived on the basis of a large amount of experimental data, is used to calculate the observation value of the particle. The importance weight of the particle is updated by comparing the value with the real strength of the electrical signal. The algorithm for self-localization, based on the MCL method with the belief function, is described in the third part in detail. Lastly, the computational cost of the proposed system is discussed.

Landmark identification

The interval between emitters allows each receiver set on the mobile robot to detect a single emitter at most. The detected emitter can be identified via its ID information. Two types of IDs are utilized in this work. The first type, which consists of multiple different frequencies, is used as the unique ID and is assigned to the IR LED array. The other type is only represented by one frequency, which is used repeatedly in the environment and is assigned to a single IR LED. The ID information is decoded by analyzing the frequencies of the signals acquired by the receiver. The received signals are easily obtained in the time domain as shown in Fig. 5a, c. The fast Fourier transform (FFT) method is used to transform the received signals into the frequency domain as shown in Fig. 5b, d.

Fig. 4 Details of the receiver. **a** Circuit of the receiver, which consists of a reverse bias circuit and non-inverting amplifier; **b** top view of the mobile robot with two photodiodes; **c** geometric relationship between the receivers and the robot in 2D space

Fig. 5 Received signals in the time and frequency domains. **a**, **c** Signals in the time domain from the unique ID encoding emitter and repeated ID encoding emitter, respectively; **b**, **d** signals in the frequency domain from the unique ID and repeated ID encoding emitters, respectively
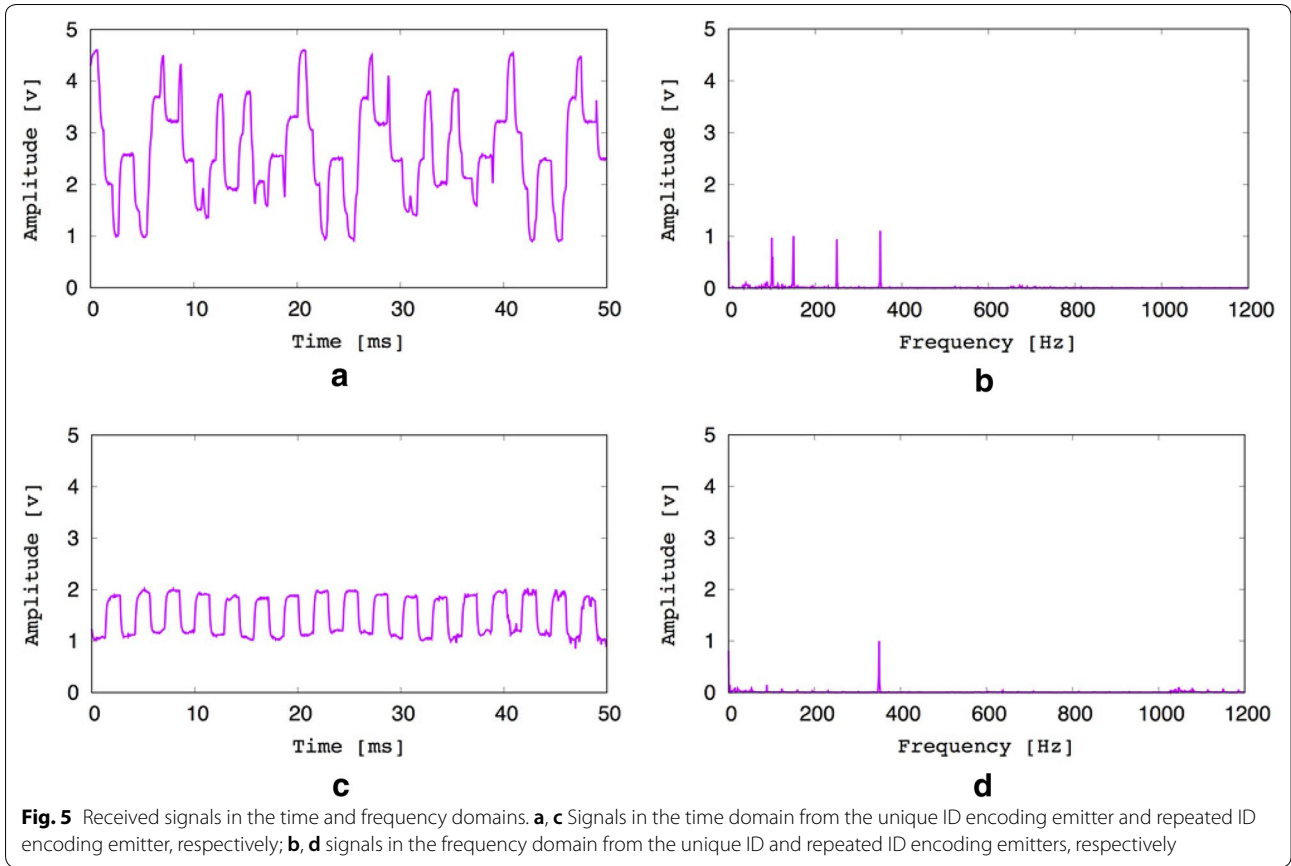
Figure 5b shows the signals received from the emitter encoded by the unique ID, which consists of four different frequencies. The unique ID encoding emitter can be directly identified by comparing the four frequencies with the ID database. Then, the position and orientation of the mobile robot are estimated based on the position of the detected emitter. Figure 5d shows the signals acquired from the emitter encoded by the repeated ID, which only contains a single frequency. As multiple emitters encoded by the same ID exist in the environment, the detected emitter cannot be identified only from the frequency of the received signal. Therefore, a belief function is proposed to determine which repeated ID encoding emitter is being detected. All the beliefs of the emitter with the detected ID are calculated by the belief function:

$$bel_n^{[l]} = \exp\left(-\frac{1}{2\sigma^2}(x_n^{[l]} - x_r)^2\right), \tag{1}$$

where $bel_n^{[l]}$ and $x_n^{[l]}$ are the belief and position of the emitter $[l]$ with the detected ID n, respectively, x_r is the position of the mobile robot, and $\sigma = 30$. The emitter with the largest value of *bel* is determined as the detected

emitter, the position of which is used for estimating the position and orientation of the mobile robot.

Calculation of the distance between the receiver and the detected emitter in the horizontal plane using the strength of the received signal

The relationship between the distance of the receiver from the detected emitter in the horizontal plane and the strength of the electrical signal is used as the observation model in this study. As for the Lambertian LED, the channel gain H of the transmitter and receiver without any filtering is given by:

$$H = \begin{cases} \frac{(m+1)A_R}{2\pi d^2}cos^m(\phi)cos(\psi), & 0 < \psi < \Psi \\ 0, & \psi > \Psi, \end{cases} \tag{2}$$

where the order m is given by $m = -\ln 2 / \ln (cos(\phi_{1/2}))$, where $\phi_{1/2}$ is the transmitter semi-angle (at half power), d is the distance from the transmitter to the receiver, A_R is the physical area covered by the photodiode, ϕ and ψ are the radiation and incidence angles with respect to the transmitter and receiver, respectively, and Ψ is the field of view (FOV) of the receiver.
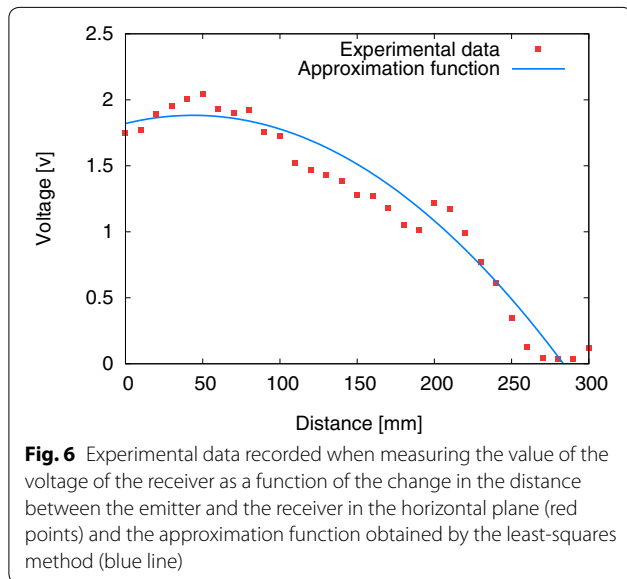
The observing noise and the loss in the circuit of the receiver always happened during the positioning procedure. Equation (2) is not able to accurately handle these additional effects. Because only one type of LED and receiver circuit is used in this system, instead of using Eq. (2), the relationship of the value of the output voltage of the receiver with the distance between the emitter and the receiver in the horizontal plane is obtained from the experimental data. These data are acquired by setting the distance between the receiver and the emitter at 1.2 m in the Z-direction in Fig. 1. The output voltage of the receiver is recorded in 10-mm intervals when the receiver moves from 0 to 300 mm in the X-direction. The experimental data are plotted in Fig. 6. The least-squares method is then used to obtain the approximation function based on these data, as shown below:

$$\overline{V} = -3.27 \times 10^{-5}|\boldsymbol{x}_p - \boldsymbol{x}_e|^2 + 2.855 \times 10^{-3}|\boldsymbol{x}_p - \boldsymbol{x}_e| + 1.81997, \tag{3}$$

where $\boldsymbol{x}_p$ denotes the position of the receiver set with the photodiode, $\boldsymbol{x}_e$ signifies the position of the detected emitter, and $\overline{V}$ indicates the value of the output voltage of the receiver with the distance between the receiver and the detected emitter in the horizontal plane. Equation (3) is used as the observation model in the positioning algorithm. The approximation function is shown in Fig. 6.

Positioning algorithm

The position and orientation of the mobile robot can be estimated based on three different landmark positions by using the trilateration method. However, this method cannot maintain other possibilities of the estimation as this would cause the estimation to become unstable.

Fig. 6 Experimental data recorded when measuring the value of the voltage of the receiver as a function of the change in the distance between the emitter and the receiver in the horizontal plane (red points) and the approximation function obtained by the least-squares method (blue line)

Therefore, in this work, the use of the MCL method with the belief function is proposed for the self-localization of the mobile robot.

Algorithm 1 Self-localization based on the MCL method with the belief function:

1: Initialize robot particles $\boldsymbol{S}_r(t) = (\boldsymbol{x}_r^{[1]}(t), \boldsymbol{x}_r^{[2]}(t), \cdots, \boldsymbol{x}_r^{[M]}(t))$
2: **for** $m = 1$ to M **do**
3:    Update particles with the motion model: $^w\boldsymbol{x}_r^{[m]}(t) = MotionModel(^w\boldsymbol{x}_r^{[m]}(t-1))$
4: **end for**
5: **if** ID n is detected **then**
6:    **if** n is a repeated ID **then**
7:       **for** $l = 1$ to L **do**
8:          update $bel_n^{[l]}$ based on the belief function
9:       **end for**
10:       update $\boldsymbol{x}_e$ based on $bel_n^{[l]}$
11:    **end if**
12:    **for** $m = 1$ to M **do**
13:       update $\omega_n^{[m]}$ based on the likelihood function
14:    **end for**
15: **end if**
16: **for** $m = 1$ to M **do**
17:    draw i with probability $\propto w_r^{[i]}(t)$
18:    add $\overline{x}_r^{[i]}(t)$ to $\overline{S}_r(t)$
19: **end for**
20: $\boldsymbol{S}_r(t) \leftarrow \overline{\boldsymbol{S}}_r(t)$
21: return $\boldsymbol{S}_r(t)$

Algorithm 1 shows the algorithm of the MCL method with the belief function. A set of particles is defined as a set of hypotheses of the robot position and orientation denoted at time t as $\boldsymbol{S}_r(t) = (\boldsymbol{x}_r^{[1]}(t), \boldsymbol{x}_r^{[2]}(t), \cdots, \boldsymbol{x}_r^{[M]}(t))$, where $[M]$ is the number of particles. First, it updates the particles representing the position and orientation of the robot by using the motion model, which is given by Eq. (4).

$$
\begin{aligned}
^w x_r(t) &= ^w x_r(t-1) + v_x \Delta t + \epsilon_x \Delta t, \epsilon_x \sim N(0, \sigma_x) \\
^w y_r(t) &= ^w y_r(t-1) + v_y \Delta t + \epsilon_y \Delta t, \epsilon_y \sim N(0, \sigma_y) \\
^w \theta_r(t) &= ^w \theta_r(t-1) + \omega \Delta t + \epsilon_\theta \Delta t, \epsilon_\theta \sim N(0, \sigma_\theta)
\end{aligned} \tag{4}
$$

where $(^w x_r^{[m]}(t), ^w y_r^{[m]}(t), ^w \theta_r^{[m]}(t))$ denotes the position and orientation of particle $[m]$ in the world coordinate, and $V = (v_x, v_y, \omega)$, and Δt indicate the velocity of the robot and period ranging from time $t - 1$ to t, respectively. A rotary encoder is installed on the motor of the wheel of the mobile robot to measure the rotational speed of the tire. The movement distance per unit of time of each tire can be calculated by utilizing the radius of the tire and converted to $(^r v_x, ^r v_y, \omega)$. Further, $N(0, \sigma)$ signifies the Gaussian distribution with standard deviation σ. As the robot is initialized without default position and orientation values being specified, the robot needs to estimate its position and orientation based on the positions of the detected emitters from the beginning. However,

emitters encoded by a repeated ID cannot be identified in the beginning without knowing the position of the robot. Therefore, the process of self-localization starts when an emitter encoded with a unique ID is detected. As shown in line 8 of Algorithm 1, if the detected ID is a repeated ID, the emitters ($[1], [2], \cdots, [L]$) encoded with this ID are assigned a *bel* by using Eq. (1). The position of the emitter with the largest *bel* is used as the input for $\boldsymbol{x}_e$ in Eq. (3) to obtain the observation value $\overline{V}$. The value of $\boldsymbol{x}_p$ is calculated based on $\boldsymbol{x}_r^{[m]}(t)$ and the geometric relationship between the receiver and the robot shown in Fig. 4c. The important weight of particle [m] is updated based on the observation value $\overline{V}$ at line 13 of Algorithm 1. The likelihood function for updating the weight of each of the particles is defined as:

$$\omega = \begin{cases} 0.001, & if \ d > \sigma \\ \beta \exp\left(-\frac{1}{2\sigma^2}(V - \overline{V})^2\right), & else, \end{cases} \quad (5)$$

where V is the value of the output voltage of the receiver when it detects the IR light. Further, d is the distance of the receiver calculated based on the position of particle [m] and the detected emitter in the horizontal plane, and σ is set as 30. Finally, resampling of the robot particles is executed based on the importance weights of these particles. The position and orientation of the robot are then estimated as the weighted mean of the particles.

$$^w\boldsymbol{x}_r(t) = \left(\frac{\Sigma_{m=1}^{M} {}^w\boldsymbol{x}_r^{[m]}(t)\omega^{[m]}}{\Sigma_{m=1}^{M} \omega^{[m]}} \right) \quad (6)$$

The procedure is subsequently repeated.

Computational cost of the proposed system

The computational cost and accuracy of the proposed system mainly depend on the number of emitters and particles used in the MCL method for self-localization. An increase in the number of particles enables the accuracy of the estimation to be improved, whereupon the computational cost also increases [33]. An alternative approach to improve the accuracy would be to use additional emitters to shorten the interval between two adjacent emitters. However, this would necessitate an increase in the memory size because of the increased number of unique IDs and would cause the computational cost to increase.

The computational cost would obviously also increase in a large environment, which would require many emitters. However, our proposed system is designed to reduce the computational cost of operating in large environments. This is a distinct advantage over the existing system, which only uses unique ID encoded emitters. For instance, our proposed system uses M particles, N_1 unique IDs, and L repeated IDs to estimate the position and orientation of the mobile robot, whereas the system that only uses unique IDs uses M particles and N_2 unique IDs. Because M new particles are created in each updating step, an update requires time in M for both systems. Moreover, the proposed and existing systems require memory size with $N_1 + L$ and N_2 to store ID information, respectively.

Expansion of the size of the environment increases both the number of repeated and unique ID encoding emitters required by our proposed system. However, the number of repeated IDs L is not changed. Only N_1 changes when the size of the environment is altered. Figure 1 shows that we use nine (L) repeated IDs and they are introduced to the ceiling with W lines in the X-direction and H lines in the Y-direction. The unique IDs are introduced between the repeated IDs as shown in Fig. 1. Then, ($W - 1$) by ($H - 1$) unique ID encoding IR emitters are needed. This indicates that the number of IDs required for our proposed method is $N_1 + L = (W - 1) * (H - 1) + 9$. If only unique IDs were used, the required number of IDs would have been $N_2 = (W - 1) * (H - 1) + W * H$. For instance, let $W = 100$ and $H = 80$, in which case $N_1 + L = 7830$ and $N_2 = 15{,}821$. Thus, the value of N_2 is more than twice that of $N_1 + L$. The utilization of a repeated ID encoding emitter reduces the increase in memory size. Furthermore, this superiority of our method is more obvious in a large environment.

Experiment

We evaluated the proposed system in the real environment. The robot used in the experiment is shown in Fig. 7. Two receivers, each equipped with a photodiode, were set on top of the mobile robot. The modulated IR LEDs were installed on the ceiling. Because of the limitations of the experimental environment, the arrangement of the emitters was adjusted relative to that in Fig. 7a to enable the proposed system to be evaluated effectively. The arrangement of the emitters used in the experiments is shown in Fig. 7b. In practice, the experimental environment comprised eight repeated ID encoding emitters and three unique ID encoding emitters that were set on the ceiling. In this work, nine different frequencies were used to generate the IDs, as listed in Table 1. All of the unique ID encoding LED arrays were generated by combining four of the nine frequencies. Therefore, each LED array consisted of four LEDs as shown Fig. 2b and each

Fig. 7 Experimental environment. **a** Illustration of the experimental environment; **b** image of the real experimental environment
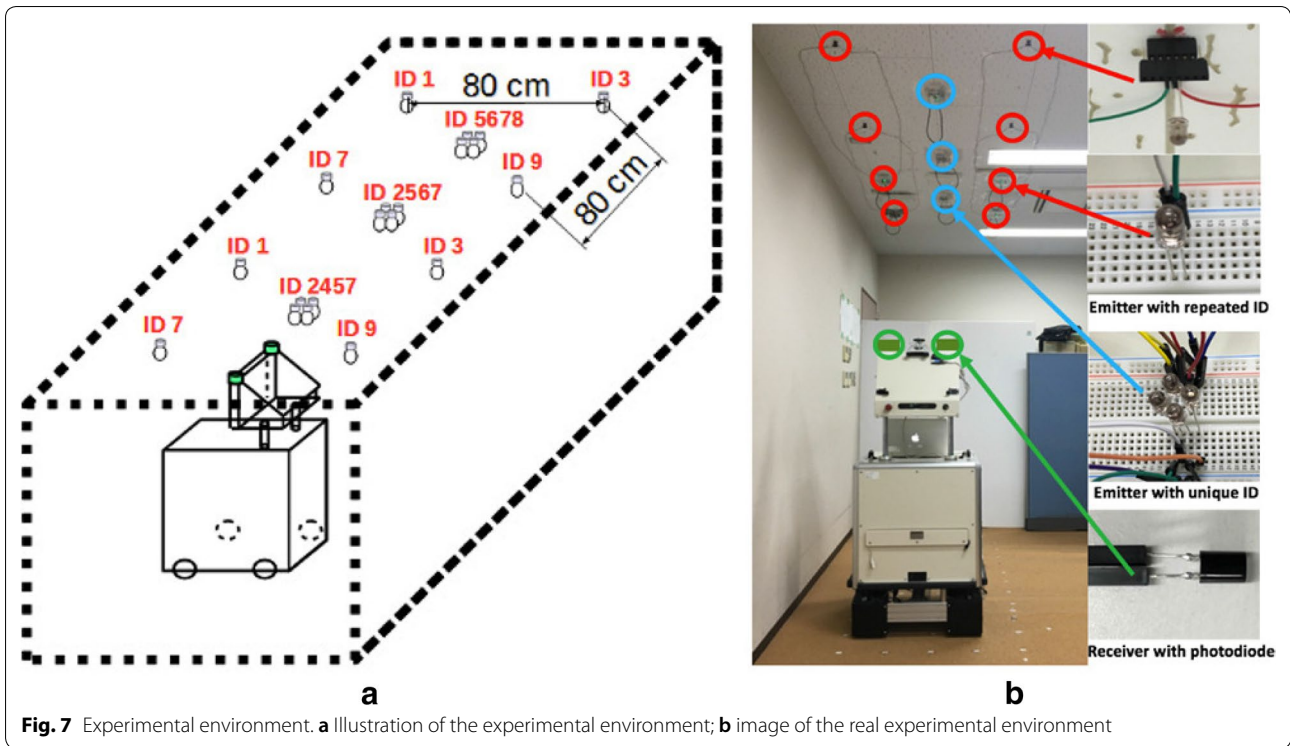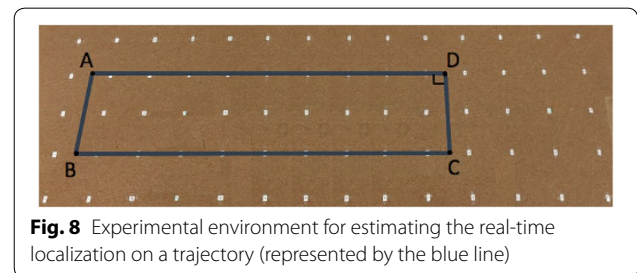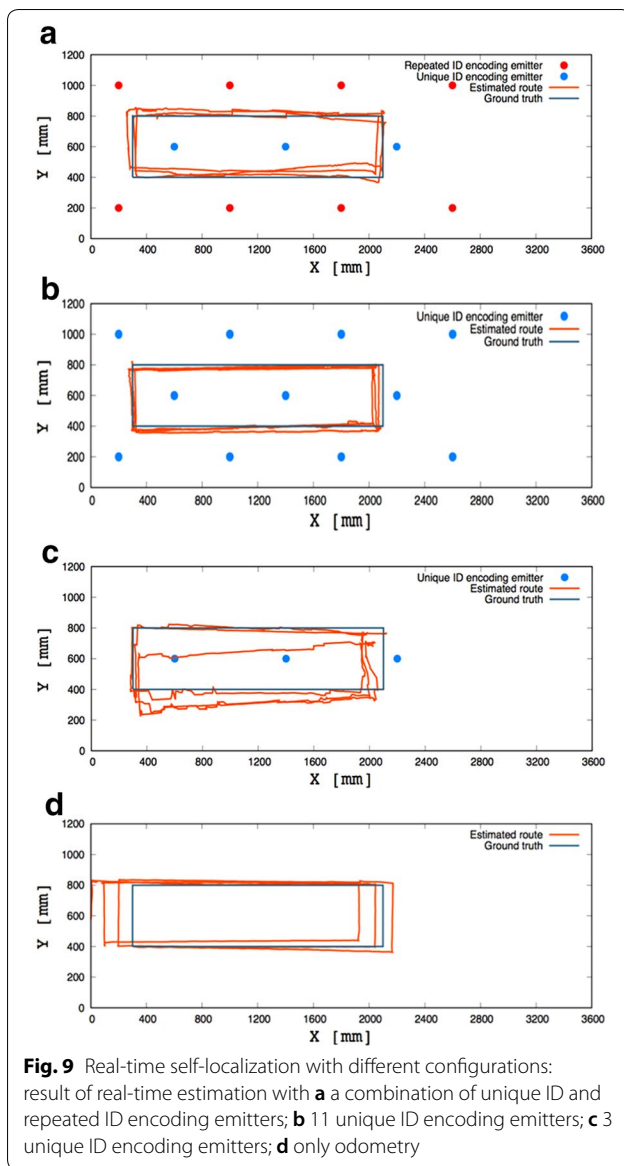
of the four LEDs is modulated with an independent frequency. Repeated ID encoding emitters consisted of one LED with a frequency that was used repeatedly. In this experiment, a total of eight microcontrollers were used, one of which was used to link with the receivers and computer to deliver the signal information and three of which were used to support the modulated signal to the three unique ID encoding emitters. The remaining microcontrollers were used for the repeated ID encoding emitters, two of which with the same ID shared one microcontroller. The height between the receiver and the emitter was set as 1.2 m.

The number of particles for estimating the robot location was set to 1000 in this experiment. In the beginning, the particles were randomly distributed in the search space of the test environment. The position and orientation of each particle were initialized by a random value within the range of the test environment. Once the particles converge, the robot performs self-localization on a trajectory or on a fixed point, enabling the robot to estimate its position and orientation accurately. Based on the position and direction of the landmark detection, the number of iterative cycles needed to converge are different. In our experiments, convergence was complete within 30 s.

Trajectory of real-time self-localization with different configurations

The uncertainty in the location of the robot increases as the interval between emitters becomes larger. In an environment in which only unique ID encoding emitters are used, attempts to improve the accuracy by decreasing the interval between the emitters causes the quantity of required IDs to increase rapidly. The proposed system, which combines unique ID encoding emitters with repeated ID encoding emitters, can reduce the interval without consuming new IDs. We verified the real-time self-localization performance of the proposed system by allowing the robot to move along fixed trajectories. This enabled us to statistically assess the real-time localization performance. The evaluation included four configurations: the combination of 3 unique ID and 8 repeated ID encoding emitters,

Fig. 8 Experimental environment for estimating the real-time localization on a trajectory (represented by the blue line)

Fig. 9 Real-time self-localization with different configurations: result of real-time estimation with **a** a combination of unique ID and repeated ID encoding emitters; **b** 11 unique ID encoding emitters; **c** 3 unique ID encoding emitters; **d** only odometry

the use of 11 unique ID encoding emitters, the use of 3 unique ID encoding emitters, and the use of no emitters. The performance assessment of self-localization under the no-emitter configuration is based only on odometry. The robot traversed the fixed trajectory three times at a set speed of 200 mm/s.

The fixed trajectory is indicated by the blue line in Fig. 8. Figure 9a–d show the results based on the aforementioned four different emitter configurations. In the case of the combined configuration, the interval between two adjacent repeated ID encoding emitters was 800 mm and the unique ID encoding emitter was positioned in the center of the square formed by four repeated ID encoding emitters, as shown in Fig. 7a. The

result of the real-time localization of the mobile robot with the combined configuration is shown in Fig. 9a. The figure shows that most of the route of the robot, as estimated by the proposed system, overlaps with the ground truth trajectory. The results confirm that the system can provide stable and accurate estimation for the mobile robot.

Because installation of the LEDs would not be entirely error free, a small deviation occurs when using Eq. (3) to describe the relationship between the output voltage of the receiver with the distance of the receiver and the detected LED in the horizontal plane. The importance of the weight updates of the particles are affected by this deviation. Therefore, incorrectly distributed particles cause the estimation of the robot location to become unstable. Especially, some of the particles were omitted because the cumulative errors of the motors were modified by the detected landmarks. These reasons gave rise to the sudden deviations and errors that occurred during the movement as shown in Fig. 9a.

Figure 9b shows the result of the self-localization using the configuration consisting of 11 unique ID encoding emitters. This configuration has the same number of emitters as the proposed combined configuration. The interval between two adjacent emitters of this configuration is also the same as that in the proposed combined configuration. The figure shows that the estimated route of the robot mostly overlaps with the ground truth trajectory. The self-localization performance is almost the same as that of the shown proposed combined configuration. However, the use of the combined configuration with the proposed method needs fewer IDs.

Figure 9c shows the result of self-localization using the configuration that consists of three unique ID encoding emitters. The interval between two adjacent unique ID encoding emitters is 800 mm. In comparison with the results obtained by using the configuration with 11 unique ID encoding emitters and the proposed combined configuration, the error is larger. The orientation of the mobile robot is incorrectly estimated during its movement and causes the estimated route to deviate from the ground truth trajectory. This can be understood by considering that an increase in the interval between the emitters prevents the robot from detecting the IR signals continuously. The motor error accumulates while the robot is moving because no landmark capable of modifying the location of the robot is detected. The particles used for estimating the robot location diverge considerably without the observation, thereby causing the accuracy of the self-localization of the mobile robot to deteriorate.

Figure 9d shows the result of self-localization based only on odometry. This result can be calculated by integrating the position of the robot and the distance covered

by the tire. The prior known position and orientation values are needed to initialize the position and orientation coordinates of the robot in the world by utilizing the odometry method. However, the prior known position and orientation values are not needed when using our proposed system. Although the routes estimated on the basis of odometry did not show the aforementioned oscillations, the motor errors accumulate considerably during movement and increase in the case of longer periods of movement.

Therefore, combining unique ID encoding emitters with repeated ID encoding emitters reduces the distance between adjacent emitters without increasing the number of new IDs. This obviously improves the accuracy of the self-localization of the mobile robot.

Localization error at fixed point of real-time self-localization

It is difficult to measure the localization error at every position along the route traversed by the robot. Therefore, we marked 70 points, indicated by the white dots shown in Fig. 10a, to evaluate the proposed system. The self-localization performance based on 11 unique ID
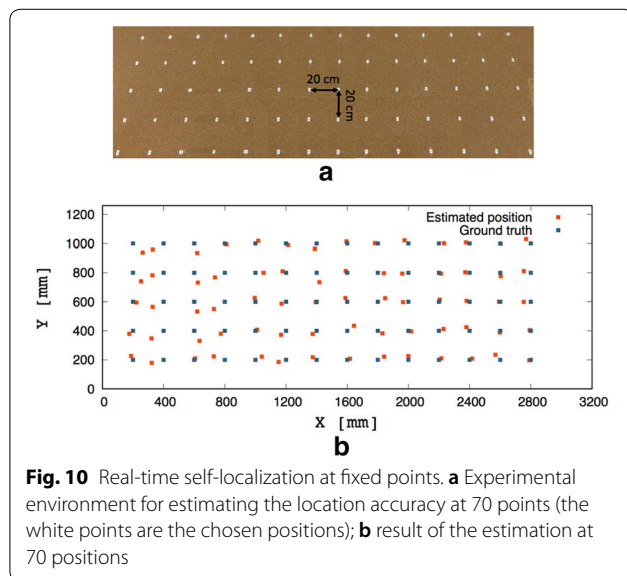
Fig. 10 Real-time self-localization at fixed points. **a** Experimental environment for estimating the location accuracy at 70 points (the white points are the chosen positions); **b** result of the estimation at 70 positions

encoding emitters, 3 unique ID encoding emitters, and odometry are also evaluated at the 70 points. The robot remained at each marked point for 3 s when passing by to perform self-localization to enable it to collect sufficient data to calculate the self-localization errors. The orientation of the robot was controlled such that it was maintained at 0 [rad].

Figure 10b compares the positions estimated by the proposed combined configuration with the true positions of the marked points. Table 2 presents the statistics of the self-localization errors on the 70 points with different configurations. The proposed combined configuration enables the robot to attain positional errors of approximately 20 mm and 30 mm in the X- and Y-directions, respectively. The average error in the estimated position is approximately 40 mm. The estimated orientation errors of the robot were calculated by comparing the estimated orientation with the real orientation 0 [rad]. The average error of the estimated orientation is approximately 0.065 [rad]. Considering the interval used for the LED configuration and the inescapable installation errors, the proposed method obtained an accurate result.

The self-localization based on 11 unique ID encoding emitters obtained the same accurate estimation as the proposed combined configuration. However, our proposed combined configuration requires fewer IDs. The self-localization performance based on both the three unique ID encoding emitters and odometry is less than satisfactory. The statistics of the self-localization errors on the 70 marked points show the same results as the evaluation on the trajectory, as shown in Fig. 9.
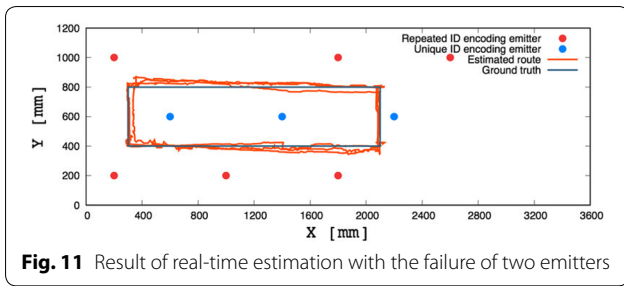
Trajectory of real-time self-localization with emitter failure

We proved the validity of the proposed system in a situation of emitter failure, which may be caused by signal occlusion, malfunction, or light decay, by evaluating the self-localization performance in an environment with emitter failures. Because the accuracy of the self-localization is closely related to the interval between emitters, the accuracy is affected by the failure of a large number of emitters. However, in our work, the emitters were installed on the ceiling as this method can be expected to minimize disturbance of the signals by obstacles.

Table 2 Self-localization errors at each of the 70 positions

Emitter configuration	Error by mean			Error by max			Variance		
	x [mm]	y [mm]	θ [rad]	x [mm]	y [mm]	θ [rad]	x [mm²]	y [mm²]	θ [rad²]
Proposed configuration	21.49	29.23	0.065	68.72	78.81	0.226	73.11	78.63	0.002
11 unique ID encoding emitters	30.17	25.28	0.041	87.09	91.22	0.100	27.55	53.61	0.001
3 unique ID encoding emitters	89.19	47.94	0.074	185.03	99.61	0.125	0.12	0.01	0.000
Odometery	93.66	54.67	0.027	160.96	98.71	0.075	0.00	0.00	0.000

Fig. 11 Result of real-time estimation with the failure of two emitters
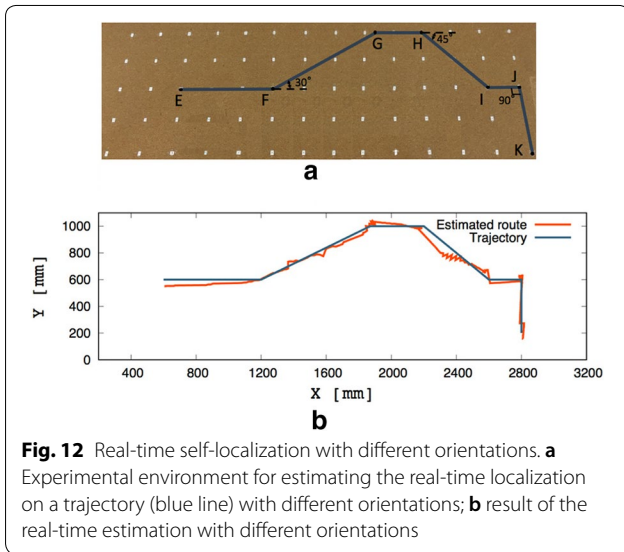
Fig. 12 Real-time self-localization with different orientations. **a** Experimental environment for estimating the real-time localization on a trajectory (blue line) with different orientations; **b** result of the real-time estimation with different orientations

highly effective, because estimation of the location of the robot can be expected to fail when its orientation is incorrectly estimated.

Figure 12b shows the result of the estimated route traversed by the mobile robot and it can be seen that the estimated route mostly overlaps with the ground truth trajectory of the experiment. Our approach allows the timely modification of the estimation errors of the position and orientation of the mobile robot. This experiment confirms that the proposed system provides a stable and accurate estimation of the self-localization of the mobile robot on a trajectory with different orientations.

Real-time self-localization with different speeds

In our experiments, in addition to setting the speed of the mobile robot at 200 mm/s, we also validated the performance of the proposed system at different speeds on the trajectory with an orientation of 0°. Figure 13 shows the real-time localization results at speeds of 100, 150, 250, and 300 mm/s, respectively. It is clear that the accuracy of the location of the robot does not decrease as the speed increases or decreases. Thus, the fast response

Emitters with different IDs are supported by independent microcontrollers and power, an arrangement designed to avoid the simultaneous failure of a large number of emitters. Therefore, in this experiment, we simulated the failure of two emitters.

Figure 11 shows the result of the self-localization in a situation in which two emitters experience failure. Compared with the configuration of emitters in Fig. 9a, two repeated ID encoding emitters are deleted from Fig. 11. As the result shows, the instability of the self-localization estimation increases. However, the accuracy is acceptable for a mobile robot.

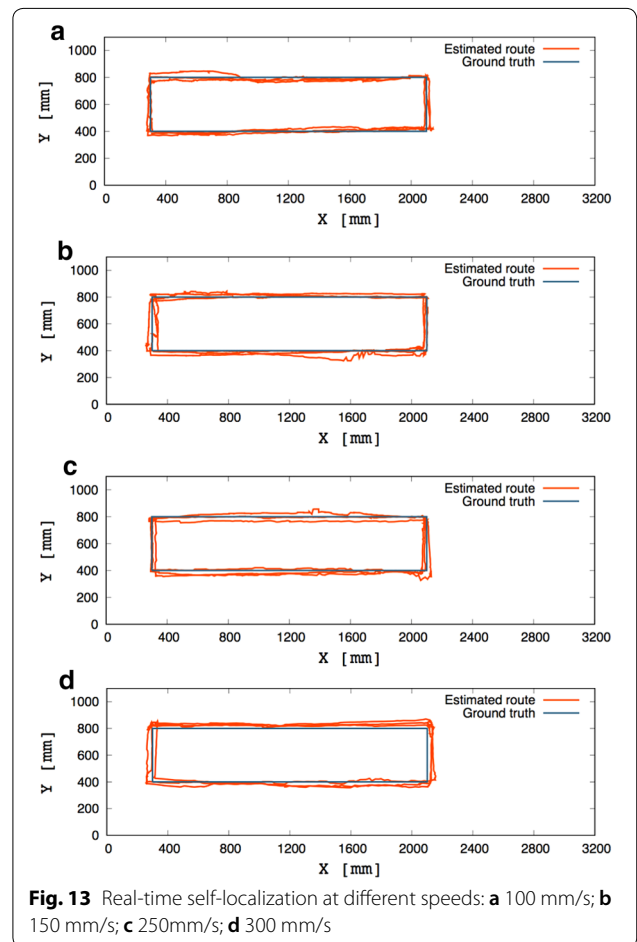**Real-time self-localization with different orientations**

The proposed system was also evaluated on another trajectory with different orientations as shown in Fig. 12a. The robot started from point E with the orientation of 0°. During the movement, the orientation of the robot changed to 30°, 45°, and 90° at points F, H, and J, respectively. This approach to evaluating the validity of the positioning system by altering the orientation of the mobile robot during its movement is

Fig. 13 Real-time self-localization at different speeds: **a** 100 mm/s; **b** 150 mm/s; **c** 250mm/s; **d** 300 mm/s

characteristics of the IR system enable it to transmit a stable signal even when the robot is moving at high speed. The errors produced by the motor and by noise are continuously compensated for by the detected emitters as shown in Fig. 13a–d.

Localization error with different heights of real-time self-localization

Equation (3), which is used as the observation model in the MCL method, is obtained at a fixed height of 120 cm between the receiver and the ceiling. The estimation of the mobile robot location is affected by errors in the height. We evaluated the effect of these errors by adjusting the height between the receiver and the ceiling from 110 to 130 cm. The self-localization of the mobile robot is performed at the marked points with these different heights.

Table 3 lists the estimation errors of the mobile robot for these different heights. The location errors in the X- and Y-directions are less than 40 mm for height changes ranging from 114 to 126 cm. The average errors of the estimated orientations are within 0.106 [rad]. The location errors obviously increase when the alteration exceeds 6 cm. Therefore, the proposed system currently lacks the ability to overcome large changes in the height of the ceiling. However, the installation errors of the emitters in the vertical direction and the undulation of the floor are commonly less than 6 cm, in which case the proposed system is unaffected by these conditions.

Conclusion and future work

This paper proposed a novel low-cost IR-system-based positioning system for the self-localization of an indoor mobile robot. IR LEDs, which emit modulated IR signals continuously, were used as active landmarks. The proposed system utilized a configuration in which unique ID encoding emitters were used in combination with repeated ID encoding emitters. The unique ID encoding emitter was an IR LED array, which was encoded by a combination of different frequencies. This combination generated additional available IDs based on a limited number of frequencies for the positioning system.

The repeated ID encoding emitter was a single IR LED encoded by repeatedly using a frequency. The combined configuration reduced the interval between two adjacent emitters without increasing the number of new IDs. Furthermore, this arrangement of emitters allowed the proposed system to be used in a large environment without being limited by the available IDs. The mobile robot was constructed by placing two receivers, each with a photodiode, on top of the robot to scan the IR signals continuously emitted by the emitters.

Self-localization of the mobile robot was realized by utilizing the MCL method with a belief function based on the prior known positions of the emitters and the strength of the IR signal detected by the receivers. Because multiple IR LEDs share the same ID, the belief function is utilized to compute the probability of each IR LED encoded by the detected ID. The LED with the largest probability was used to calculate the observation value for updating the importance weight of each particle. The mobile robot can estimate its location without knowing its starting position and orientation. The experimental results, which were obtained in a real environment, confirmed the validity of the proposed system.

The proposed system generates additional IDs by utilizing a combined configuration. This novel configuration combines unique ID encoding landmarks with repeated ID encoding landmarks to improve the estimation accuracy and reduce the production, ID, and computational costs. Especially, the proposed configuration is suitable for positioning systems based on other sensors. A disadvantage of the proposed system is that the prior knowledge used for estimation of the mobile robot is prepared by hand, which incurs some inescapable artificial errors. Equation (3) was obtained for a fixed height of the ceiling. This indicates that the proposed system is currently unable to perform accurately when the height of the ceiling changes.

In our future work, we expect to replace the human work to obtain prior knowledge by the simulations localization and mapping (SLAM) method. A combination of SLAM method proposed in [33] with the RSS fingerprints method is considered necessary to complete this work. The use of the SLAM method is expected to

Table 3 Self-localization errors with different heights

Height [cm]	110	112	114	116	118	*120*	122	124	126	128	130
Error by mean											
x [mm]	53.45	74.36	37.94	28.47	25.01	*21.49*	26.36	36.02	21.82	87.43	55.82
y [mm]	60.07	41.75	30.22	37.66	25.67	*29.23*	28.05	29.90	36.10	20.61	51.04
θ [rad]	0.204	0.118	0.103	0.106	0.042	*0.065*	0.051	0.011	0.062	0.036	0.073
Error by max											
x [mm]	128.56	141.37	103.25	56.23	44.76	*68.72*	52.65	62.84	50.26	121.85	97.65
y [mm]	215.58	96.28	76.27	88.44	38.10	*78.81*	46.67	73.92	72.14	39.07	76.68
θ [rad]	0.221	0.160	0.158	0.147	0.077	*0.226*	0.067	0.022	0.084	0.053	0.114

Italic values indicate significance of results at the standard height of 120 cm

solve the installation error and the problem presented by changes in the height of the ceiling. The proposed system currently supports accurate estimation in 2D space; however, the system is also scalable for 3D positioning, in which case additional receivers and sensors would be required. The proposed system is also foreseen to be used for the positioning of people in indoor environments. In this case, the receiver is the camera of a mobile phone, which analyzes the frequency information of the signal transformed from the emitter. The positions of people can be estimated based on the positions of the detected emitters.

Authors' contributions
JW was the main contributor to this work. YTs contributions include the basic idea, mathematical formulation, and discussion of the proposed method. Both authors read and apprvoed the final manuscript.

Publisher's Note

References

1. Jekabsons G, Kairish V, Zuravlyov V (2011) An analysis of wi-fi based indoor positioning accuracy. Appl Comput Syst 44(1):131–137. https://doi.org/10.2478/v10143-011-0031-4
2. Biswas J, Veloso M (2010) Wifi localization and navigation for autonomous indoor mobile robots. In: 2010 IEEE international conference on robotics and automation, pp 4379–4384. https://doi.org/10.1109/ROBOT.2010.5509842
3. Galvan CE, Galvan-Tejada I, Sandoval EI, Brena R (2012) Wifi bluetooth based combined positioning algorithm. Proc Eng 35:101–108
4. Raghavan AN, Ananthapadmanaban H, Sivamurugan MS, Ravindran B (2010) Accurate mobile robot localization in indoor environments using bluetooth. In: 2010 IEEE international conference on robotics and automation, pp 4391–4396. https://doi.org/10.1109/ROBOT.2010.5509232
5. Yayan U, Yucel H, Yazıcı A (2015) A low cost ultrasonic based positioning system for the indoor navigation of mobile robots. J Intell Robot Syst 78(3):541–552. https://doi.org/10.1007/s10846-014-0060-7
6. Hwang KH, Kim DE, Lee DH, Kuc TY (2006) A simple ultrasonic gps system for indoor mobile robot system using kalman filtering. In: Proceedings of the 2006 SICE-ICASE international joint conference, pp 2915–2918. https://doi.org/10.1109/SICE.2006.314996
7. Cho SH, Hong S (2010) Map based indoor robot navigation and localization using laser range finder. In: 2010 11th international conference
8. on control automation robotics vision, pp 1559–1564. https://doi.org/10.1109/ICARCV.2010.5707420
8. Wang Z, Hwang YS, Kim YK, Lee DH, Lee J (2015) Mobile robot indoor localization using surf algorithm based on lrf sensor. In: 2015 54th annual conference of the society of instrument and control engineers of Japan (SICE), pp 1122–1125. https://doi.org/10.1109/SICE.2015.7285500
9. Mi J, Takahashi Y (2015) Performance analysis of mobile robot self-localizaiton based on different configurations of rfid system. In: 2015 IEEE international conference on advanced intelligent mechatronics (AIM), July 7–11, 2015, Busan, Korea, pp 1591–1596
10. Park S, Hashimoto S (2009) Indoor localization for autonomous mobile robot based on passive rfid. In: 2008 IEEE international conference on robotics and biomimetics, pp 1856–1861. https://doi.org/10.1109/ROBIO.2009.4913284
11. Lee J, Hyun CH, Park MA (2013) A vision-based automated guided vehicle system with marker recognition for indoor use. Sensors 13(8):10052–10073. https://doi.org/10.3390/s130810052
12. Hijikata S, Terabayashi K, Umeda K (2009) A simple indoor self-localization system using infrared leds. In: 2009 sixth international conference on networked sensing systems (INSS), pp 1–7. https://doi.org/10.1109/INSS.2009.5409955
13. Bae J, Lee S, Song J-B (2008) Use of coded infrared light for mobile robot localization. J Mech Sci Technol 22(7):1279–1286
14. Mao L, Chen J, Li Z, Zhang D (2013) Relative localization method of multiple micro robots based on simple sensors. Int J Adv Robot Syst 10(2):128. https://doi.org/10.5772/55587
15. Luo P, Zhang M, Zhang X, Cai G, Han D, Li Q (2013) An indoor visible light communication positioning system using dual-tone multi-frequency technique. International workshop on optical wireless communications (IWOW)
16. Qiu K, Zhang F, Liu M (2015) Visible light communication-based indoor localization using Gaussian process. In: 2015 IEEE/RSJ international conference on intelligent robots and systems (IROS), pp 3125–3130. https://doi.org/10.1109/IROS.2015.7353809
17. Oh JH, Kim D, Lee BH (2014) An indoor localization system for mobile robots using an active infrared positioning sensor. J Ind Intell Inf 2(1):35–38
18. Lee S (2009) Use of infrared light reflecting landmarks for localization. Ind Robot Int J 36(2):138–145. https://doi.org/10.1108/01439910910932595
19. Krejsa J, Vechet S (2012) Infrared beacons based localization of mobile robot. Elektronika ir Elektrotechnika 117(1):17–22
20. Chen CH, Song KT (2005) Complete coverage motion control of a cleaning robot using infrared sensors. In: IEEE international conference on mechatronics, 2005. ICM '05, pp 543–548. https://doi.org/10.1109/ICMECH.2005.1529316
21. Gfeller FR, Bapst U (1979) Wireless in-house data communication via diffuse infrared radiation. In: Proceedings of the IEEE 67(11), pp 1474–1486. https://doi.org/10.1109/PROC.1979.11508
22. Thrun S, Burgard W, Fox D (2006) Probabilistic robotics. The MIT Press, Cambridge
23. Mautz R, Tilch S (2011) Survey of optical indoor positioning systems. In: 2011 international conference on indoor positioning and indoor navigation, pp 1–7. https://doi.org/10.1109/IPIN.2011.6071925
24. Nuaimi KA, Kamel H (2011) A survey of indoor positioning systems and algorithms. In: 2011 international conference on innovations in information technology, pp 185–190. https://doi.org/10.1109/INNOVATIONS.2011.5893813
25. Koyuncu H, Yang SH (2010) A survey of indoor positioning and object locating systems. IJCSNS Int J Comput Sci Netw Secur 10(5):121–128
26. Liu H, Darabi H, Banerjee P, Liu J (2007) Survey of wireless indoor positioning techniques and systems. IEEE Trans Syst Man Cybern Part C Appl Rev 37(6):1067–1080. https://doi.org/10.1109/TSMCC.2007.905750
27. Desouza GN, Kak AC (2002) Vision for mobile robot navigation: a survey. IEEE Trans Pattern Anal Mach Intell 24(2):237–267. https://doi.org/10.1109/34.982903
28. robotshop: Hagisonic StarGazer RS robot localization system. http://www.robotshop.com/en/hagisonic-stargazer-rs-localization-system.html
29. Ul-Haque I, Prassler E (2010) Experimental evaluation of a low-cost mobile robot localization technique for large indoor public environments. In: ISR 2010 (41st international symposium on robotics) and ROBOTIK 2010 (6th German conference on robotics), pp 1–7

30. Lee S, Song JB (2007) Use of coded infrared light as artificial landmarks for mobile robot localization. In: 2007 IEEE/RSJ international conference on intelligent robots and systems, pp 1731–1736. https://doi.org/10.1109/IROS.2007.4399600

31. Gorostiza EM, Lázaro Galilea JL, Meca Meca FJ, Salido Monzú D, Espinosa Zapata F, Pallarés Puerto L (2011) Infrared sensor system for mobile-robot positioning in intelligent spaces. Sensors 11(5):5416–5438. https://doi.org/10.3390/s110505416

32. Wang J, Takahashi Y (2017) A low-cost light based self-localization system with repeated landmark id for the indoor mobile robot. In: The 5th international workshop on advanced computational intelligence and intelligent informatics (IWACIII 2017)

33. Wang J, Takahashi Y (2017) Slam method based on independent particle filters for landmark mapping and localization for mobile robot based on hf-band rfid system. Journal of Intelligent & Robotic Systems. https://doi.org/10.1007/s10846-017-0701-8